Light Absorption Mechanism of c-Si/*a*-Si Half-Coaxial Nanowire Arrays for Nanostructured Heterojunction Photovoltaics

Xia Hua, Yang Zeng, Weizhou Wang, and Wenzhong Shen

***Abstract*— We theoretically studied the assembly of horizontal single crystalline-silicon (c-Si)/amorphous-silicon (*a*-Si) core/shell nanowires (NWs) into c-Si/*a*-Si half-coaxial NW arrays (NWAs), which can be realized in large size for c-Si/*a*-Si heterojunction solar cells. Through the finite-difference time-domain simulations, we investigated the absorption mechanism of the half-coaxial scheme. The single building block of half-coaxial NWAs owns strong leaky mode resonances, which are the key for NWs to exceed the planar absorption limit. These resonances can be well preserved in the NWAs, leading to an excellent absorption enhancement. We further carefully studied the influences of various structural factors, i.e., the light interaction effect of periodic arrays, leaky mode resonances in single blocks, and the effect of indium tin oxide coatings. The optimized half-coaxial NWAs are capable of absorbing most of the incident light with only 10-μm thick c-Si substrate. Thus, the half-coaxial proposal can significantly cut the required c-Si wafer thickness in heterojunction solar cells, which loosens the restriction on material quality of the c-Si substrate. This half-coaxial NWAs structure may serve as a new way to improve the efficiency and reduce the cost of silicon heterojunction solar cells.**

***Index Terms*— Light trapping, nanowires (NWs), photovoltaic cells, semiconductor device modeling, semiconductor nanostructures.**

I. Introduction

OVER the past decade, silicon nanowires (NWs) have emerged as one promising platform to explore the high-efficiency and cost-effective solar cells due to their unique absorption properties resulted from the subwavelength dimension [1]–[8]. The coaxial heterostructure NWs of a crystalline-silicon (c-Si) core and an amorphous-silicon (*a*-Si) shell have been proposed as potential photovoltaic building blocks [2], [6], [9] as they combine the advantages of the long charge carrier diffusion lengths of c-Si and the high absorption coefficient of *a*-Si [6], [10], [11]. Meanwhile, the *a*-Si shell is capable of simultaneously providing effective surface passivation for c-Si and creating a p-n heterojunction with better band structure to enhance the open-circuit voltage (V_{OC}) [12]. The charge separation along the radius in the radial c-Si/*a*-Si junction also increases the defect tolerance [13]. Researchers have both numerically and experimentally exhibited the extremely high light absorption and photocurrent density of the single c-Si/*a*-Si coaxial NWs compared with c-Si NWs [6], [9].

Nevertheless, the single NWs can only serve as nanoscale power sources [3], hence it is essential to consider the assembling and scaling of these individual c-Si/*a*-Si NWs into arrays for general purpose solar cells [1]. Several groups have made beneficial attempts on the c-Si/*a*-Si core/shell vertically oriented NW arrays (V-NWAs) [2], [10], [13]–[18], which stand vertically with the axial direction perpendicular to the substrate plane. This kind of integration produces excellent antireflection and absorption properties due to the resonator antenna effect. However, the performances of the 2-D V-NWAs-based solar cells are typically limited by a fundamental tradeoff between the attainable optical absorption and the concomitant severe electrical recombination, since the surface area is unavoidably dramatically amplified by very long NWs [13], [14]. Recently, the 1-D horizontally oriented NWAs (H-NWAs) [1], [4], [15] have attracted much interest as another prospective assembly strategy. Different from the V-NWAs, the H-NWAs lie flat on the substrate with the axial direction parallel to the substrate plane, in which the resonance effect is much stronger than in the V-NWAs [13]. This is because the resonances in V-NWAs can be excited only by scattered light, while the resonances in H-NWAs can be excited directly by incident light. Cao *et al.* [3], [4] used the leaky mode resonances (LMRs) to study the resonance effect in H-NWAs, which resemble a whispering gallery mode in a nanoscale cavity. The LMRs are the key for H-NWAs to break the planar absorption limits, and are widely adopted by many researchers to explore the diverse exciting advantages of the horizontal design, such as enlarged optical

Manuscript received May 14, 2014; revised October 9, 2014; accepted October 10, 2014. Date of publication October 23, 2014; date of current version December 9, 2014. This work was supported in part by the National Major Basic Research Project under Grant 2012CB934302 and in part by the National Natural Science Foundation of China under Grant 11174202, Grant 61234005, and Grant 11474201. The review of this paper was arranged by Editor A. G. Aberle.

X. Hua is with the Laboratory of Condensed Matter Spectroscopy and Opto-Electronic Physics, Key Laboratory of Artificial Structures and Quantum Control, Department of Physics and Astronomy, Institute of Solar Energy, Ministry of Education, Shanghai Jiao Tong University, Shanghai 200240, China, and also with the Gansu Electric Power Research Institute, State Grid Gansu Electric Power Company, Lanzhou 730050, China (e-mail: huax@sjtu.edu.cn).

Y. Zeng and W. Shen are with the Laboratory of Condensed Matter Spectroscopy and Opto-Electronic Physics, Key Laboratory of Artificial Structures and Quantum Control, Department of Physics and Astronomy, Institute of Solar Energy, Ministry of Education, Shanghai Jiao Tong University, Shanghai 200240, China (e-mail: zephyrus_z@sjtu.edu.cn; wzshen@sjtu.edu.cn).

W. Wang is with the Gansu Electric Power Research Institute, State Grid Gansu Electric Power Company, Lanzhou 730050, China (e-mail: 1157639917@qq.com).

Color versions of one or more of the figures in this paper are available online at http://ieeexplore.ieee.org.

Digital Object Identifier 10.1109/TED.2014.2363001

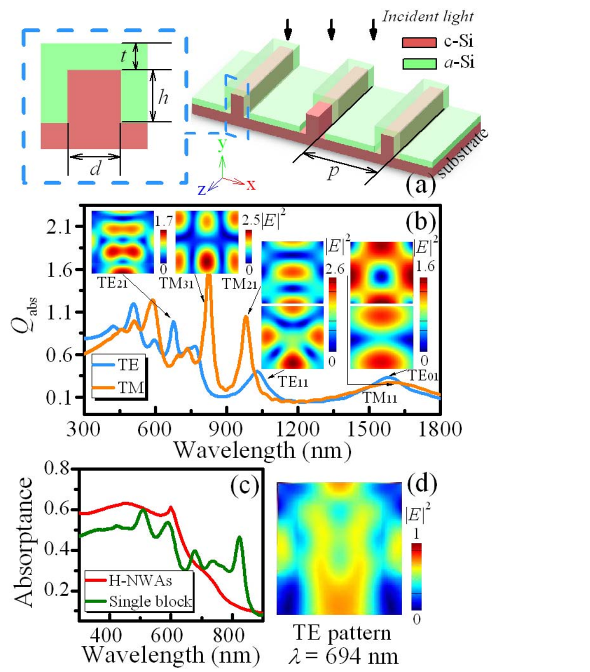

Fig. 1. (a) Schematic c-Si (core)/*a*-Si (shell) half-coaxial NWAs (right) and an enlarged single building block (left). (b) Calculated spectra of Q_{abs} versus wavelength under TM (TE) polarized illumination. Insets: distribution of the electric filed intensity normalized to incident light for the corresponding peaks indicated by arrows. (c) Absorption spectra for the half-coaxial H-NWAs and single building block. (d) Distribution of the electric field intensity normalized to incident light at wavelength $\lambda = 694$ nm under TE illumination.

cross section, broadband antireflection, angle-independence, and material saving [1], [3]–[9], [15], [16]. Nonetheless, most of these advanced designs involve complex and expensive synthesis, which even offsets their optical superiorities and can only be realized in a few periods [1], [7].

So far, a few studies have referred to the horizontal assembly of c-Si/*a*-Si coaxial NWs or their unique optical properties due to the dissimilar materials of the core and shell. In this paper, we try to find a feasible and potential assembly strategy of c-Si/*a*-Si core/shell NWs. Based on the previous studies of H-NWAs, we propose the c-Si/*a*-Si half-coaxial NWAs as a simple and general integration strategy for the large-area high performance solar devices, which can be realized by standard patterning and deposition techniques. We have demonstrated that the structure of c-Si (core)/*a*-Si (shell) NWs lying flat on a c-Si substrate [Fig. 1(a)] can effectively preserve the LMRs excited within single NW elements. Combining the LMRs and total light interaction effect of periodic arrays, we obtain very strong absorption enhancement in the half-coaxial NWAs. We also give fundamental insights of the influences of structural parameters and coatings for further optimization. As a result, the best half-coaxial NWAs structure can absorb most of the incident light with only 10-μm thick c-Si substrate. Moreover, we apply the half-coaxial NWAs to the heterojunction with intrinsic thin (HIT) layer solar cell and cut the required substrate thickness to about 10 μm, which is significantly thinner than the traditionally used wafers. The reduction of c-Si substrate thickness makes cheap wafers of low quality acceptable in the fabrication of high-efficiency heterojunction solar cells.

II. Modeling Details

We have performed the finite-difference time-domain (FDTD) simulations [19] to obtain the light absorption in all structures throughout this paper. Fig. 1(a) shows the schematic plot of the c-Si (core)/*a*-Si (shell) half-coaxial NWAs structure, with an enlarged sketch of the single building block in the left dash box. The half-coaxial NWs structure is formed by integrating the c-Si/*a*-Si coaxial NWs onto the underneath c-Si substrate, which lies flat on the substrate and turns the perfect coaxial structure into half-coaxial. The half-coaxial NWAs can be prepared by standard thin film deposition of the *a*-Si shell on the patterned c-Si substrate, and are characterized by the c-Si core diameter d, the core height h, the *a*-Si shell thickness t, and the period of arrays p, as marked in Fig. 1(a). For the single NW building block of the half-coaxial NWAs, we have employed a simulation box of $0.6(x) \times 0.6(y) \times 1(z)$ μm with perfectly matched layer conditions in x-and y-direction, and periodic boundary condition in z-direction [see the axis in Fig. 1(a)]. Thus, we can treat the single building block as infinitely long, which has been well applied to describing the light scattering and absorbing of various single NWs [4], [5]. The incident light source is a broadband (300–1800 nm) plane wave normal to the substrate (along the y-axis). The mesh grid is set to be 2 nm over the entire simulation region. The absorbed power is directly calculated using frequency-domain transmission monitors positioned around the absorbing volume. A 2-D frequency-domain field monitor cross cutting the building block in its center in the xy plane is used to calculate the electric field intensity distribution [discussed later in the insets of Fig. 1(b)]. The complex refractive indices n and k are picked from [11], which are widely adopted in solar device modeling [5], [6], [20]. The FDTD dispersion model is Lorentz–Drude model.

For the NWAs structures studied in Figs. 1(c) and (d) and 2–4, the FDTD calculation utilize a simulation box of $p(x) \times 2(y) \times 0.7(z)$ μm with periodic boundary conditions in x- and z-direction, and perfectly matched layer condition in y-direction. The reflected power R and transmitted power T normalized to the incident light power are obtained through the frequency-domain transmission monitors positioned at the bottom and top of simulation region in xz plane. The absorbed power is calculated as $A = 1 - R - T$. Other modeling parameters follow the same with single NW building blocks as stated above.

III. Results and Discussion

We show the schematic plot of the half-coaxial NWAs in Fig. 1(a). The half-coaxial NWAs structure is very different from the H-NWAs in [1]–[4], since it involves the c-Si and *a*-Si core/shell structure and attaches to the underneath substrate. The proposed half-coaxial NWAs naturally own unique optical properties because of the dissimilar absorbing materials of the core and shell. We start from the optical

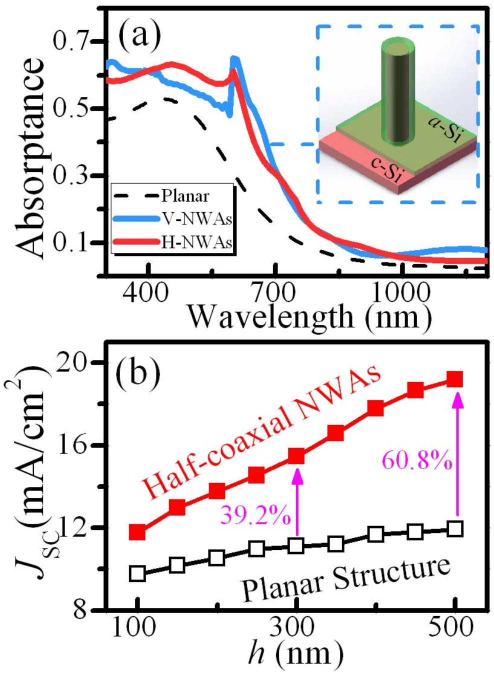

Fig. 2. (a) Absorption spectra for the H-NWAs with h = 200 nm, V-NWAs with h = 300 nm and planar structures with h = 200 nm. Inset: schematic plot of the V-NWAs. (b) h dependence of J_{SC} for the half-coaxial NWAs and planar structures.

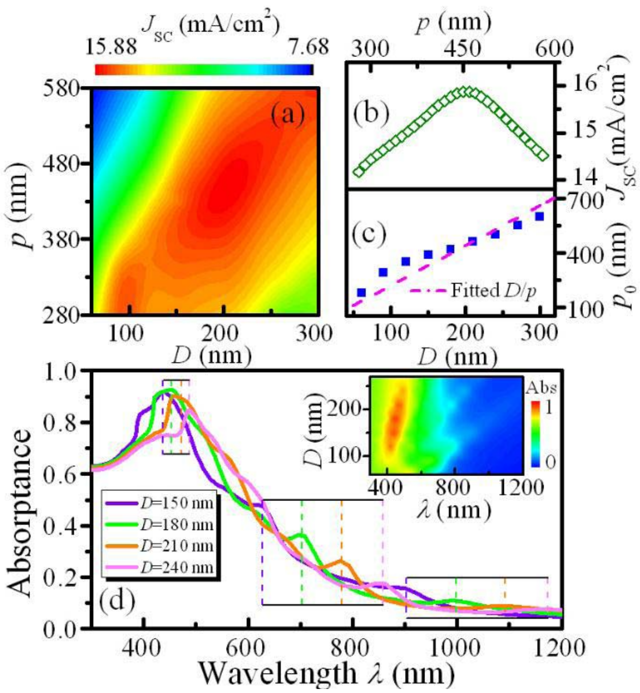

Fig. 3. (a) 2-D plot of J_{SC} as a function of period p and diameter of single building block D ($D = d + 2t$). (b) p dependence of J_{SC} under D = 210 nm. (c) Best period p_0 versus D. (d) Absorption spectra for varied D = 150, 180, 210, and 240 nm. Inset: 2-D plot of absorptance as a function of wavelength λ and D ranging from 60 to 280 nm.

properties of the single building block of the half-coaxial NWAs to give some fundamental insights. Since the single building block is transformed from cylindrical NWs and is attached to the c-Si substrate, the absorption performance

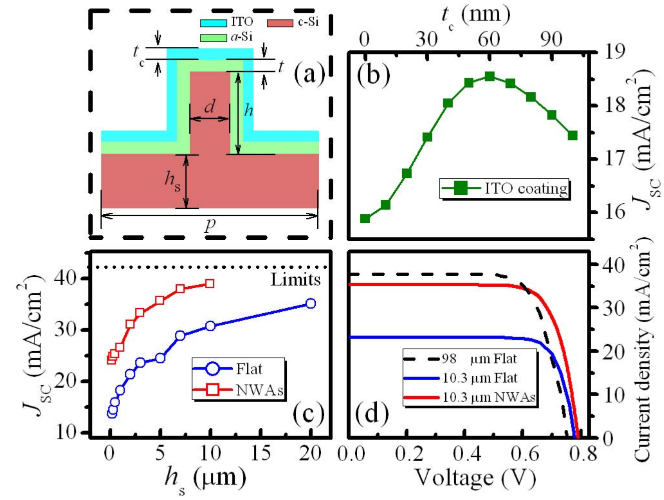

Fig. 4. (a) Cross section drawn of the half-coaxial NWAs with ITO coating and c-Si substrate. (b) J_{SC} versus ITO coating thickness t_c. (c) Achievable J_{SC} with varied h_s for the half-coaxial NWAs and flat structure. (d) J–V curves of flat structure HIT solar cell with 98-μm thick c-Si wafer, flat structure HIT solar cell with 10.3-μm thick c-Si wafer, and half-coaxial NWAs structure HIT solar cell with 10.3-μm thick c-Si wafer, under AM1.5 solar spectrum.

may be different from that of traditional cylindrical NWs. We demonstrate the changed absorption properties of this single building block in Fig. 1(b) by calculating the spectra of the absorption efficiency Q_{abs}, i.e., the absorption cross section normalized to the geometrical cross section [4]–[6]. The structural parameters of the half-coaxial building block are $d = h = 200$ nm and $t = 50$ nm. Note that for unpolarized sunlight $Q_{\mathrm{abs}} = (Q_{\mathrm{abs}}^{\mathrm{TM}} + Q_{\mathrm{abs}}^{\mathrm{TE}})/2$, where $Q_{\mathrm{abs}}^{\mathrm{TM}}$ and $Q_{\mathrm{abs}}^{\mathrm{TE}}$ denote absorption efficiencies for transverse magnetic [(TM), electric field parallel to NWs axial direction] and transverse electric [(TE), electric field perpendicular to axial direction] illuminations, respectively. We can clearly observe the distinct resonant peaks corresponding to the LMRs of different orders as indicated to be TE/TM$_{m,l}$ in Fig. 1(b) [3]. Except the lowest order mode TE$_{01}$ and TM$_{11}$, most of these resonances occur in the wavelength range of 400–1000 nm, leading to great potentials for photovoltaics since the wavelength region covers the main part of the AM1.5 solar spectrum. We have also presented the internal electric field distributions of the LMRs in the insets of Fig. 1(b). These resonance patterns are very similar to the typical TE/TM modes patterns demonstrated in [3] and [6], with a small observed shift toward the c-Si substrate. This can be interpreted as the break of the perfect light confinement within NWs and the light coupling into the substrate. Thus, we can confirm that the LMRs are also the dominant light trapping in the half-coaxial single building block morphology, which is the key for H-NWAs to obtain strong absorption.

Then, we expand the single building block into arrays to form the c-Si/*a*-Si half-coaxial NWAs. This proposed structure serves as a simple and general assembly solution of single NWs for practical solar devices, and can be easily realized through standard technologies of thin film deposition of the *a*-Si shell on the patterned c-Si substrate. Specifically, the nanoscale patterned substrate may be prepared in centimeter scale by various conventional nanolithography methods such as nanoimprint lithography with a resolution of <200 nm [21]. The cost is lower than that of the more advanced technologies that have higher resolutions of <100 nm, and may be further cut down with technology development. The following deposition of the *a*-Si shell can be completed through plasma-enhanced or hot wire chemical vapor deposition, both of which are low-cost and proven techniques for large-size deposition. The fabrication difficulty mainly lies in the surface control of the patterned c-Si. The clean and even surface plays a crucial role in uniform deposition of *a*-Si film, especially when the *a*-Si film is ultrathin. Thus, the surface maintenance should be very careful when moving samples to film deposition after nanopatterning process. Compared with those complicated assembly strategies limited to a few periods [1], [7], the NWAs is attainable on an area of several inches, which is a relatively large size for the nanostructure-based photovoltaics [22] because of the homogeneousness issue.

In Fig. 1(c), we calculate the absorption spectrum of the half-coaxial NWAs with the same parameters as that of the single building block ($d = h = 2004$ nm and $t = 50$ nm). The period of NWAs p is set as 600 nm without much optimization. Note that here we treat the c-Si substrate as infinitely thick without any back surface reflection and do not consider the absorption of the substrate. The absorption spectrum of the single building block of the NWAs under unpolarized illumination is also shown in Fig. 1(c) for comparison. We can see that in short-wavelength region (300–800 nm), the absorption of NWAs is quite comparable with that of the single building block, while the absorption resonant peaks are predictably merged because of the influence of the light interaction effect in periodic arrays (discussed later in Fig. 3). The observation that the absorption spectra of NWAs become flat compared with that of the single building block is consistent with the literature results [4], [9], primarily due to the off-resonance absorption enhancement from light dispersion and interaction in periodic arrays. On the other hand, in long wavelength region (>800 nm), the absorption of NWAs loses the resonant peaks because the lower order LMRs (TM_{21}/TE_{11} and TM_{11}/TE_{01}) are much more sensitive to substrate coupling and extend further out of the NWs into the underlying c-Si substrate [3]. Nevertheless, its influence is limited since the AM1.5 spectrum declines to very weak in that long wavelength region. We further demonstrate in Fig. 1(d) the TE pattern at the wavelength $\lambda = 694$ nm to directly see the remaining LMRs. The TE pattern corresponding to TE_{21} of the single building block [see the inset of Fig. 1(b)] appears very similar to the original TE_{21} pattern, but with a shift to the substrate below arisen from light coupling. From Fig. 1(d), we can infer the preservation of the LMRs in the NWAs, which play a crucial role in the absorption properties [as discussed later in Fig. 3(d)].

To see the absorption superiority of the proposed half-coaxial NWAs, we compare the absorption spectra between the half-coaxial NWAs and the planar structure with the same $h = 200$ nm and $t = 50$ nm in Fig. 2(a). We can find that the absorption of the half-coaxial NWAs achieves significant increment in the wavelength range of 300–800 nm, benefiting from the well-preserved strong LMRs and light interaction in periodic arrays. On the other hand, the absorption shows little improvement (<10%) for long wavelengths because of the strong coupling to the substrate, as shown in Fig. 1(c). Next, we give out the comparable absorption spectrum of the vertically oriented c-Si/*a*-Si NWAs [see the schematic plot in the inset of Fig. 2(a), and the NWs are typical cylinders as commonly prepared] with the same $d = 200$ nm and $t = 50$ nm, but a higher $h = 300$ nm. Obviously, the half-coaxial NWAs with smaller NW length exhibit very close absorption spectrum compared with the V-NWAs and even obtain ~10% enhancement in the wavelength range of 400–600 nm, which is the most important spectral range of the AM1.5 spectrum. More importantly, the surface area of the half-coaxial NWAs is only 5/9 of that of the V-NWAs, implying a greatly reduced surface recombination for the NWAs-based solar cells. Therefore, compared with the vertically oriented designs, the horizontally oriented half-coaxial NWAs own great prospects to realize high-efficiency nanostructured photovoltaics, because of the achievable excellent light absorption with substantially decreased structure height and surface area.

The absorption of the half-coaxial NWAs can be engineered by various structural factors. The higher h naturally leads to enhanced light absorption, which has been commonly observed in diverse nanostructures [10]. Fig. 2(b) shows out the integrated short-circuit current density J_{SC} of the half-coaxial NWAs with varied h ($d = 200$ nm, $t = 50$ nm, and $p = 600$ nm as figured above). Note that the J_{SC} is calculated over the AM1.5 spectrum (from 300 nm to the bandgap of the absorbing materials, i.e., 1107 nm for c-Si and 712 nm for *a*-Si) without any electrical loss as $J_{SC} = q \int \Gamma(\lambda)\mathrm{Abs}(\lambda) d\lambda$, where q is the elementary charge, Γ is the photon flux density, and $\mathrm{Abs}(\lambda)$ denotes the absorption of the structure as a function of wavelength λ. This J_{SC} of 100% internal quantum efficiency is commonly used in nanostructured photovoltaics to characterize the absorption ability of the structure [4]–[6], [9], [11]. The h-dependent J_{SC} of the planar structure with the same $t = 50$ nm is also shown for comparison. We can see that the J_{SC} considerably increases with increasing h because of the prolonged optical path length and increased absorbing volume. The enhancement of J_{SC} compared with the planar structure also grows with increasing h to 39.2% at $h = 300$ nm, and even reaches 60.8% at $h = 500$ nm with the extremely high $J_{SC} = \sim 20$ mA/cm^2. Considering that $h = 500$ nm would result in greatly enlarged surface area and subsequently severe surface recombination loss, here we pick $h = 300$ nm as our best choice, which already provides satisfactory optical absorption.

Fig. 3(a) shows the influences of other structural factors, i.e., the period p, the c-Si core diameter d as well as the *a*-Si thickness t, on the calculated J_{SC} of the proposed half-coaxial NWAs. It should be clarified that we have fixed $d/t = 4/1$ in all our simulations to simplify the material proportion issue, and have used the diameter of the single building block $D = d + 2t$ to replace d for a clearer description on size impacts. First, it is found that J_{SC} always ascends with increasing p until the peak value and then declines sharply [see the p-dependence of J_{SC} under $D = 210$ nm in Fig. 3(b)], which corresponds closely to the results in [4]. This behavior comes from the total light interaction effect of the periodic arrays, which is to some extent similar to the light coupling and propagations within the 1-D gratings-based structures [23], [24]. The Rayleigh anomaly [25] and Febry-Pérot phase-matching resonances originated from the coupling of Bloch modes [23], [24], which comprehensively determine the light absorption in the periodic configuration. In addition, we also find that the best period p_0 under different D appears to be approximately linear to D [as indicated in Fig. 3(c)], which can be used to roughly evaluate the suitable values of p and D for reference.

On the other hand, different from the 1-D gratings, the absorption enhancement of NWAs is not only determined by the periodicity, but also the single building blocks with core/shell structure. The D plays a crucial role in absorption properties because it dominates the LMRs in every single building block of the half-coaxial NWAs. In Fig. 3(a), the J_{SC} shows a fluctuating trend with increasing D and obtains the best values in the region of $D = 150$–240 nm. We plot in Fig. 3(d) the absorption spectra of varied D from 150 to 240 nm to see the detailed change of the resonances in the structure. We can observe three evident resonant peaks in the wavelength range of 300–1200 nm corresponding to the LMRs of single building block, as shown in Fig. 1(b). Clearly, the resonances red-shift with increasing D as indicated by dashed lines, and the D-driven red-shift substantially grows larger for longer wavelength, which matches well with the behavior of LMRs in single NWs [4]–[6]. The shift of the resonant peak around the wavelength of 1000 nm can reach up to 280 nm between $D = 150$ nm and $D = 240$ nm. Moreover, we present the 2-D plot of absorptance in the inset of Fig. 3(d) to see the change of absorption with different wavelength for a larger range of D. It is found that the three evident resonances red-shift with increasing D, and the resonance intensities gradually shrink when the resonant peaks red-shift to longer wavelength. This absorption behavior is in good accordance with the calculated result in [3] on single NWs, which also confirms the preservation of the LMRs in the half-coaxial NWAs. Consequently, the D determines not only the absorption peak position but also the resonance intensity, leading to the optimal $J_{SC} = 15.88$ mA/cm^2 at $D = 210$ nm ($d = 140$ nm, $t = 35$ nm, and $p = 460$ nm). It should be noted that very large D (>300 nm) can support more LMRs modes [5], [6], but the resonances may red-shift beyond the wavelength of 1200 nm (1.03 eV that is lower than the bandgap of c-Si), and have no contribution to the photogenerated current.

On the basis of the above systematical investigation and optimization of the light interaction in periodic arrays and the LMRs in single building blocks, we further introduce the indium tin oxides (ITOs) coating and c-Si substrate in the half-coaxial NWAs, as schematically shown in Fig. 4(a), which are generally adopted in realistic photovoltaics. The ITO coating is an indispensable component of heterojunction solar cells both for its high conductivity and optical benefits. The influence of ITO coating thickness t_c on the J_{SC} of the half-coaxial NWAs with the optimal configuration presented above ($D = 210$ nm, $p = 460$ nm, and $h = 300$ nm) is shown in Fig. 4(b). We have not considered the absorption of ITO in the simulation because of its large bandgap (3.9 eV). Critically, the absorption performance improves with increasing t_c until the peak $J_{SC} = 18.55$ mA/cm^2 at $t_c = 60$ nm and then degrades for thicker t_c. This thickness dependence is similar to the behavior of antireflection coating on traditional planar structure, since the half-coaxial NWAs contain a large area of flat part. However, it should be pointed out that the optimal t_c may vary with different D because the ITO coating also perturbs the LMRs for the Fano interface effect in NWs [5] and the change of effective refractive index of the environment.

With the optimal $t_c = 60$-nm thick ITO coating, we turn to calculate the attainable J_{SC} with different substrate thickness h_s in Fig. 4(c) to explore the absorption ability of the half-coaxial NWAs. Note that here the substrate is no longer treated as infinitely thick and the absorption of the substrate is included in the calculation, while no reflective back contact is applied at the back surface. To compare with the conventional c-Si/$a-$Si heterojunction solar cell such as HIT solar cell, here we choose $t = 25$ nm [correspondingly, $d = 100$ nm, $D = 150$ nm, and $p = 390$ nm, as obtained in Fig. 3(a)], which is the generally adopted a-Si layer thickness. The J_{SC} of a flat structure with corresponding h_s (the total thickness is $h + h_s$) under the same 60-nm thick ITO coating and the theoretical limit are given as references. The J_{SC} of the half-coaxial NWAs appears dramatic increase between $h_s = 0$ and 2 μm, and gradually grows after 2 μm until saturating at 10 μm. Compared with the flat condition, the J_{SC} of the half-coaxial NWAs structure keeps substantial enhancement for all h_s. The NWAs structure with $h_s = 10$ μm can even provide much higher J_{SC} than the flat structure with $h_s = 20$ μm, achieving an extremely high J_{SC} of nearly 40 mA/cm^2, which approaches closely to the theoretical limit. Subsequently, we can tell that the half-coaxial NWAs structure with only 10-μm thick substrate is capable of absorbing most part of incident sun light. Actually, for Panasonic's HIT solar cell structure [26], a 98-μm thick c-Si substrate with extra light trapping is necessary to absorb most of the incident light and produce satisfactory current. Therefore, the half-coaxial NWAs not only suppress the front surface reflection like other antireflection textures, but also significantly reduce the required minimum thickness of c-Si substrate due to the enhanced absorption, resulting in numerous benefits to improve the performance of solar devices.

Finally, we extend the half-coaxial NWAs structure into HIT solar cells to see the advantages brought by thinner c-Si substrate. In Fig. 4(d), we employ the AFORS-HET (numerical simulator automat for simulations of heterojunction) [27] to calculate the J–V curves of three differently structured HIT solar cells: p-a-Si (10 nm)/i-a-Si (15 nm)/n-c-Si (98 μm) flat structure, p-a-Si (10 nm)/i-a-Si (15 nm)/n-c-Si (10.3 μm) flat structure, and p-a-Si (10 nm)/i-a-Si (15 nm)/n-c-Si (10.3 μm) NWAs-based structure. The half-coaxial NWAs here use the same parameters in Fig. 4(c) for comparison ($D = 150$ nm, $p = 390$ nm, $h = 300$ nm, and $h_s = 10$ μm). The incident illumination is set as AM1.5 spectrum and a 60-nm thick ITO coating is applied in all three structures. The p-type doping concentration is 7.5×10^{19} cm^{-3}, while the contacts are assumed as metal/semiconductor Schottky contact and flat-band. The elaborate defect states distribution model of the c-Si and a-Si bulk, c–Si/a–Si interface are picked from [27] and [28], which is based on the reported experimental results. The defect states in a-Si layer are exponential bandtail states and Gaussian distributed deep dangling-bond states, while the defects in c-Si wafer are acceptor-like oxidation vacancy. The interface defect states are Gaussian distributed with the peak located at midgap of c-Si, and do not result in modified band bending. The defect states distribution model determines the recombination of the solar cell simulation. All other required electrical parameters are all referred to [27, Table I] to ensure the reliability.

For the flat structure HIT solar cell with 98-μm thick c-Si, we obtain the $V_{\mathrm{OC}} = 0.753$ V, $J_{\mathrm{SC}} = 37.81$ mA/cm^2, fill factor FF = 74.80%, and conversion efficiency $\eta = 21.30\%$. Comparing the simulated results with Panasonic's reported data of experimental HIT solar cell ($V_{\mathrm{OC}} = 0.75$ V, $J_{\mathrm{SC}} = 39.5$ mA/cm^2, FF = 83.2%, and $\eta = 24.7\%$) [26], we can see that the simulation is reasonable. Although there are certain discrepancies between the exact numbers of J_{SC} and FF due to the usage of additional new technologies and very high quality c-Si wafers in the experiment, this simulation setup is sufficient to show the key concept in the following, i.e., the gain in cell performance that comes with a much thinner substrate. When we reduce the flat c-Si substrate thickness to 10.3 μm (including $h = 300$ nm and $h_s = 10$ μm), the J_{SC} and η dramatically decline, suffering from the incomplete light absorbing, as shown in Fig. 4(c). However, the V_{OC} rises to 0.779 V because of ~90% cut of c-Si, which leads to a substantial decrease of bulk recombination. Note that in practice this rise in V_{OC} may be compensated by the increase in the surface recombination that comes with the passivation and homogeneousness issues. Then, we replace the flat c-Si substrate with the half-coaxial NWAs structure of the same thickness 10.3 μm (with $h = 300$ nm and $h_s = 10$ μm). We can find that the yielded J_{SC} grows back to 35.34 mA/cm^2, benefiting from the excellent light absorption of the half-coaxial NWAs as discussed above. The improvements of V_{OC} and FF that come from the reduced bulk recombination and resistance remain at the same level. As a result, the half-coaxial NWAs-based HIT solar cell with only 10.3-μm thick c-Si wafer achieves an $\eta = 21.65\%$, which is 0.35% higher than that of the 98-μm thick simulated flat structure HIT solar cell, showing a new way to realize ultrathin high-efficiency solar cells ($\eta > 20\%$ with <50-μm thick silicon absorbing layer [29]). More importantly, the largely reduced substrate thickness requirement mkes cheaper silicon wafers with lower qualities feasible in high-efficiency solar devices, since the diffusion length of ~10 μm is enough within such a thin silicon layer.

IV. Conclusion

We have proposed the c-Si/a-Si half-coaxial NWAs as an easy and general assembly strategy of single c-Si (core)/a-Si (shell) NWs, which is potentially scalable to large-area modules by standard patterning and deposition technologies. We have employed the FDTD simulations to illustrate that the half-coaxial scheme attached to a c-Si substrate effectively retains the LMRs within the single elements, providing satisfactory absorption with small structure height and surface area. Detailed optimization has been achieved by carefully tuning the influences of light interaction in periodic arrays and the LMRs in single blocks as well as the ITO coating. As a result, the half-coaxial NWAs structure is able to absorb most of the incident light with only 10-μm c-Si substrate, much thinner than the conventional thickness of ~98 μm for planar structured HIT solar cell. This reduction of necessary substrate thickness of HIT solar cell yields improved solar cell performance benefiting from the accompanying decline of the bulk recombination and resistance. The thinner substrate may also be a new method to cut the cost of silicon heterojunction solar cells due to the loosened restrictions on material quality of the c-Si substrate.

References

[1] T. J. Kempa, R. W. Day, S.-K. Kim, H.-G. Park, and C. M. Lieber, "Semiconductor nanowires: A platform for exploring limits and concepts for nano-enabled solar cells," *Energy Environ. Sci.*, vol. 6, no. 3, pp. 719–733, Jan. 2013.

[2] M. M. Adachi, M. P. Anantram, and K. S. Karim, "Optical properties of crystalline–amorphous core–shell silicon nanowires," *Nano Lett.*, vol. 10, no. 3, pp. 4093–4098, Sep. 2010.

[3] L. Cao, J. S. White, J.-S. Park, J. A. Schuller, B. M. Clemens, and M. L. Brongersma, "Engineering light absorption in semiconductor nanowire devices," *Nature Mater.*, vol. 8, no. 8, pp. 643–647, Aug. 2009.

[4] L. Cao *et al.*, "Semiconductor nanowire optical antenna solar absorbers," *Nano Lett.*, vol. 10, no. 2, pp. 439–445, Feb. 2010.

[5] W. F. Liu, J. I. Oh, and W. Z. Shen, "Light trapping in single coaxial nanowires for photovoltaic applications," *IEEE Electron Device Lett.*, vol. 32, no. 1, pp. 45–47, Jan. 2011.

[6] W. F. Liu, J. I. Oh, and W. Z. Shen, "Light absorption mechanism in single c-Si (core)/a-Si (shell) coaxial nanowires," *Nanotechnology*, vol. 22, no. 2, pp. 125705–125709, Feb. 2011.

[7] B. Tian *et al.*, "Coaxial silicon nanowires as solar cells and nanoelectronic power sources," *Nature*, vol. 449, no. 7164, pp. 885–889, Oct. 2007.

[8] M. L. Brongersma, Y. Cui, and S. Fan, "Light management for photovoltaics using high-index nanostructures," *Nature Mater.*, vol. 13, no. 5, pp. 451–460, May 2014.

[9] B. Tian, T. J. Kempa, and C. M. Lieber, "Single nanowire photovoltaics," *Chem. Soc. Rev.*, vol. 38, no. 1, pp. 16–24, Jan. 2009.

[10] W. Q. Xie, W. F. Liu, J. I. Oh, and W. Z. Shen, "Optical absorption in c-Si/a-Si:H core/shell nanowire arrays for photovoltaic applications," *Appl. Phys. Lett.*, vol. 99, no. 3, p. 033107, Jul. 2011.

[11] E. D. Palik, *Handbook of Optical Constants of Solids*. London, U.K.: Academic, 1985.

[12] M. Taguchi *et al.*, "HIT^{TM} cells–high-efficiency crystalline Si cells with novel structure," *Prog. Photovolt., Res. Appl.*, vol. 8, no. 5, pp. 503–513, Sep./Oct. 2000.

[13] E. C. Garnett, M. L. Brongersma, Y. Cui, and M. D. McGehee, "Nanowire solar cells," *Annu. Rev. Mater. Res.*, vol. 41, pp. 269–295, Aug. 2011.

[14] B.-R. Huang, Y.-K. Yang, T.-C. Lin, and W.-L. Yang, "A simple and low-cost technique for silicon nanowire arrays based solar cells," *Solar Energy Mater. Solar Cells*, vol. 98, pp. 357–362, Mar. 2010.

[15] D. Tham and J. R. Heath, "Ultradense, deep subwavelength nanowire array photovoltaics as engineered optical thin films," *Nano Lett.*, vol. 10, no. 11, pp. 4429–4434, Nov. 2010.

[16] F. Proise *et al.*, "InP-based nano solar cells," *Proc. SPIE*, vol. 8981, p. 89811G, Mar. 2014.

[17] M. Foldyna, L. Yu, S. Misra, and P. R. I. Cabarrocas, "Using nanowires to enhance light trapping in solar cells," *SPIE Newsroom*, Nov. 2013.

[18] M. Zanuccoli *et al.*, "Numerical simulation of vertical silicon nanowires based heterojunction solar cells," *Energy Proc.*, vol. 38, pp. 216–222, Sep. 2013.
[19] *FDTD Solutions 8.0*, Lumerical, Vancouver, BC, Canada, 2012.
[20] P. Spinelli, M. A. Verschuuren, and A. Polman, "Broadband omnidirectional antireflection coating based on subwavelength surface Mie resonators," *Nature Commun.*, vol. 3, no. 2, p. 692, Feb. 2012.
[21] P. N. Prasad, *Nanophotonics*. New York, NY, USA: Wiley, 2004.
[22] X. X. Lin, X. Hua, Z. G. Huang, and W. Z. Shen, "Realization of high performance silicon nanowire based solar cells with large size," *Nanotechnology*, vol. 24, no. 23, p. 235402, May 2013.
[23] P. Lalanne, J. P. Hugonin, and P. Chavel, "Optical properties of deep lamellar gratings: A coupled Bloch-mode insight," *J. Lightw. Technol.*, vol. 24, no. 6, pp. 2442–2449, Jun. 2006.
[24] S. Bandiera, D. Jacob, T. Muller, F. Marquier, M. Laroche, and J.-J. Greffet, "Enhanced absorption by nanostructured silicon," *Appl. Phys. Lett.*, vol. 93, no. 19. p. 193103, Nov. 2008.
[25] L. Rayleigh, "Note on the remarkable case of diffraction spectra described by Prof. Wood," *Philosoph. Mag.*, vol. 14, no. 79, pp. 60–65, Jun. 1907.
[26] M. Taguchi *et al.*, "24.7% record efficiency HIT solar cell on thin silicon wafer," *IEEE J. Photovolt.*, vol. 4, no. 1, pp. 96–99, Jan. 2014.
[27] X. Hua, Z. P. Li, W. Z. Shen, G. Y. Xiong, X. S. Wang, and L. J. Zhang, "Mechanism of trapping effect in heterojunction with intrinsic thin-layer solar cells: Effect of density of defect states," *IEEE Trans. Electron Devices*, vol. 59, no. 5, pp. 1227–1235, May 2012.
[28] S. Zhong, X. Hua, and W. Shen, "Simulation of high-efficiency crystalline silicon solar cells with homo–hetero junctions," *IEEE Trans. Electron Devices*, vol. 60, no. 7, pp. 2104–2110, Jul. 2013.
[29] D. Kray and K. R. McIntosh, "Analysis of ultrathin high-efficiency silicon solar cells," *Phys. Status Solidi A*, vol. 206, no. 7, pp. 1647–1654, May 2009.

Xia Hua received the bachelor degree in physics from Shanghai Jiao Tong University, China, in 2009. He received Ph.D. degree in semiconductor physics from the Department of Physics and Astronomy, Shanghai Jiao Tong University from the Department of Physics and Astronomy, Shanghai Jiao Tong University, China, in 2014.

He is currently working in the Gansu Electric Power Research Institute, Lanzhou, China.

Yang Zeng was born in Chengdu, China, in 1988. He received the bachelor's degree in physics from Shanghai Jiao Tong University, Shanghai, China, in 2010, where he is currently pursuing the Ph.D. degree with the Department of Physics and Astronomy.

His current research interests include semiconductor physics and solar cells.

Weizhou Wang was born in Lintao, China, in 1967.

He is currently the Vice President of the Gansu Electric Power Research Institute, Lanzhou, China, and the Director of the Laboratory for the Loss Reduction and Energy Saving Technology. He is also the Senior Engineer and an Engineering Technologist with the State Grid Electric Power Company, Lanzhou.

Wenzhong Shen was born in Suzhou, China, in 1968. He received the Ph.D. degree in semiconductor physics and semiconductor device from the Chinese Academy of Sciences, Beijing, China, in 1995.

He has been the Director of the Key Laboratory of Artificial Structures and Quantum Control, Ministry of Education, Shanghai Jiao Tong University, Shanghai, China, since 2009.